AIP | Review of Scientific Instruments

Interactive optical design and realization of an optimized charge coupled device Thomson scattering system for the spherical tokamak START

M. J. Walsh, N. J. Conway, M. Dunstan, M. J. Forrest, and R. B. Huxford

Citation: Rev. Sci. Instrum. **70**, 742 (1999); doi: 10.1063/1.1149436
View online: http://dx.doi.org/10.1063/1.1149436
View Table of Contents: http://rsi.aip.org/resource/1/RSINAK/v70/i1
Published by the American Institute of Physics.

Related Articles

Fourier transform infrared absorption spectroscopy characterization of gaseous atmospheric pressure plasmas with 2 mm spatial resolution
Rev. Sci. Instrum. 83, 103508 (2012)

Kr II laser-induced fluorescence for measuring plasma acceleration
Rev. Sci. Instrum. 83, 103111 (2012)

Laser schlieren deflectometry for temperature analysis of filamentary non-thermal atmospheric pressure plasma
Rev. Sci. Instrum. 83, 103506 (2012)

Reconstruction of polar magnetic field from single axis tomography of Faraday rotation in plasmas
Phys. Plasmas 19, 103107 (2012)

Study of the plasma wave excited by intense femtosecond laser pulses in a dielectric capillary
Phys. Plasmas 19, 093121 (2012)

Additional information on Rev. Sci. Instrum.

Journal Homepage: http://rsi.aip.org
Journal Information: http://rsi.aip.org/about/about_the_journal
Top downloads: http://rsi.aip.org/features/most_downloaded
Information for Authors: http://rsi.aip.org/authors

ADVERTISEMENT

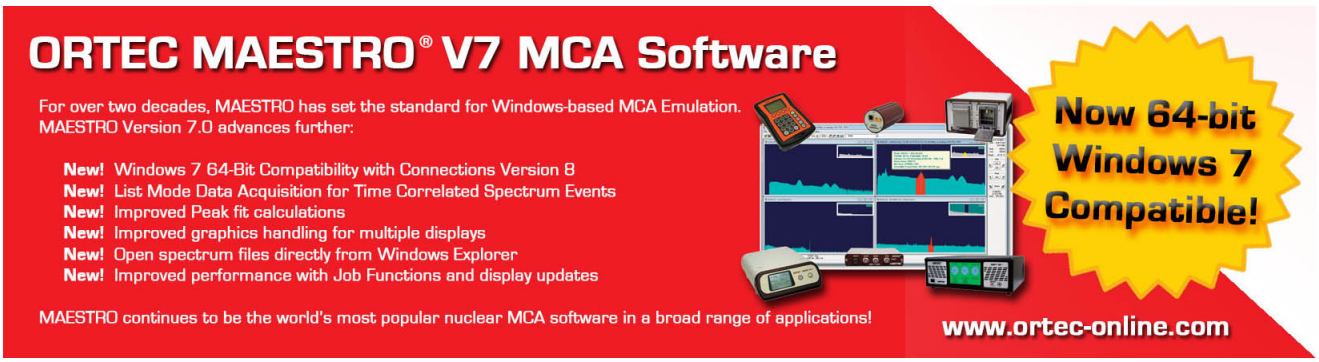

Interactive optical design and realization of an optimized charge coupled device Thomson scattering system for the spherical tokamak START

M. J. Walsh
Walsh Scientific Ltd., Culham Sciene Centre, Abingdon, Oxon OX14 3EB, United Kingdom

N. J. Conway
University College Dublin, Dublin, Ireland

M. Dunstan and M. J. Forrest
UKAEA Fusion, Culham Science Centre, Abingdon, Oxon, OX14 3DB, United Kingdom

R. B. Huxford
RBH Optics, Burgess Hill, West Sussex RH15 8HL, United Kingdom

(Presented on 9 June 1998)

A high resolution, multipoint Thomson scattering system has been successfully implemented on the START tokamak. It incorporates a low-divergence, 10–15 J *Q*-switched ruby laser system with a gated (GaAs) image intensifier (II) and a charge coupled device as the detection elements. It is designed to measure temperatures between 25 eV and 4 keV and densities from 3×10^{18} m^{-3} with high accuracy ($\sim$2.5%). The spatial resolution is approximately 1.5 cm. An interactive design of the optics train has been used to ensure matching of the optics from light collection to light detection. Use of coherent fiber bundles allows a resolution down to about 2 mm. © *1999 American Institute of Physics.* [S0034-6748(99)69301-7]

I. INTRODUCTION

Recent work on the tight aspect ratio tokamak START[1] has indicated several favorable features in the areas of confinement, transport, stability, and operational limits. These have warranted further detailed studies of internal profiles, in particular of the electron temperature and density profiles. The design specifications for the system were to measure electron temperatures in the range of 25 eV to 4 keV and electron densities of greater than 3×10^{18} m^{-3}.

In this article, the design of a multipoint Thomson scattering system is detailed. The system is in the TV category as characterized by Bretz *et al.*[2] and Barth *et al.*[3] The philosophy of the design was to transfer the maximum possible scattered light from the scattering volume to the detector without compromising the system performance in terms of efficiency, optical cross talk, and light gathering power. Obtaining the highest photon throughput has involved the use of high aperture lenses (e.g., f/0.7) and spectrometer slits of height equal to that of the grating. This presented severe design problems which were solved by using interactive optical design techniques and optimizing the optical system as a whole from collection optics to charge coupled device (CCD) (image intensifier) rather than the different optical stages separately.

II. OUTLINE DESIGN

In this system, scattering angles of 83° to 116° are required from a 600 mm length of laser beam (15 J, 0.4 mrad divergence, ruby) in the plasma midplane, using a large diameter lens assembly mounted close to the START vacuum vessel (see Fig. 1). This is imaged onto coherent fiber bundles each channel collecting light from a 15 mm$\times$3.5 mm scattering volume and a nominal f/6 light cone. The light is then transported by the fibers (12 m) and coupled to a relay lens (see Fig. 2). This lens directs the light through a short wavelength blocking filter in a telecentric lens system and onto a diffraction grating via Littrow lens. The dispersed light travels back through the Littrow lens to an intermediate image plane. The spatial channels can be seen in the vertical dimension (five are shown for illustration). Then the light is guided via a spherical-field mirror to a very high performance image intensifier lens (f/0.71) whose final element is in optical contact with the image intensifier. After the image intensifier, the light is coupled to a CCD camera and then processed by a computer. The overall system is automated to produce a complete profile of electron temperature and density for each laser pulse.

III. COLLECTION LENS

The prime function of the objective lens is the efficient collection of scattered radiation from the laser beam and matching this to the f/1.75 acceptance angle of the fibers. The vignetting of less than 10% across the field of view (FOV) is achieved by positioning the field stop at the first surface of the objective. The residual vignetting is caused by limitations of the viewing window, i.e., aperture, vacuum vessel obstructions, and the oblique angle of the window to the optical axis.

After due consideration of alternatives such as the Double Gauss, Petzval, and Catadioptric configurations which were rejected for reasons of stop location, FOV coverage, and size restriction around the vacuum vessel, the chosen design is based on a triplet derivative construction.[4] The front lens is split into two elements, to enhance the aperture

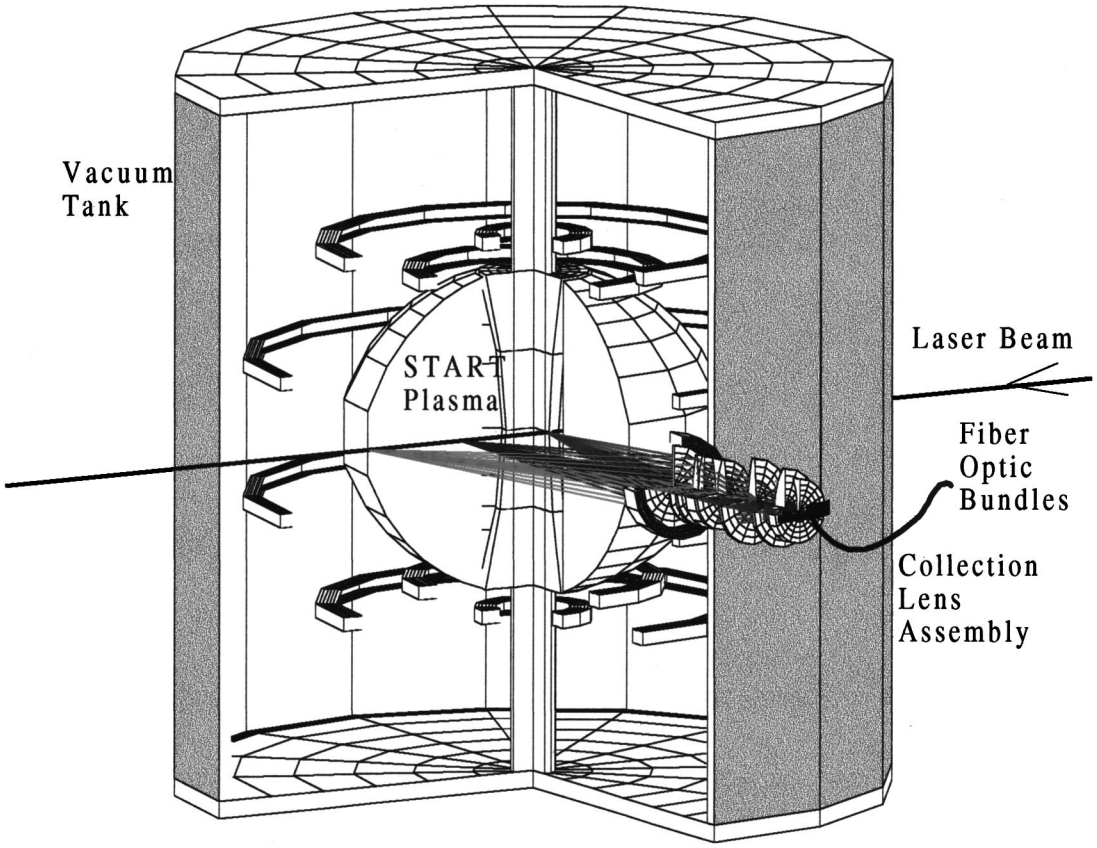

FIG. 1. START vessel showing layout of laser and collection system.

performance, while the off axis performance is maintained by a combination of a field flattener and an image surface which is concave to the objective. The field flattener also corrects the lateral chromatic aberration and directs the principal rays such that they are normal to the image surface. The tilted object (laser beam) is catered for by a corresponding tilt of the image surface. The combination of all these techniques gives a uniform performance across the entire FOV.

IV. SPECTROMETER

The object plane, containing 40 fiber bundles, each 1.02 mm high by 4.3 mm wide, is oriented to provide a straight image on the detector in both wavelength and space. A 1 m spectrometer with f/6 input necessitates a slit height of ~160 mm high (this is shown graphically in Fig. 3). The fiber bundles are rotated such that the long side of the fiber bundle is across the input slit. This allows the number of channels to be maximized on one detector (i.e., image intensifier/CCD system). Because of the geometry of the intensifier/CCD arrangement, the output slit has maximum dimensions of 163 mm ~163 mm in the midplane (see Fig. 3). This accommodates the wavelength range of 680–820 nm which covers the temperature range of 25 eV to 4 keV and allows calibration using Rayleigh scattering.

The spectrometer is based on the Littrow design (see Fig. 2). This facilitates correction for aberrations introduced by the use of very high input slits. The light path in the spectrometer has two intermediate images before being finally imaged at f/0.71 onto the intensifier photocathode. In

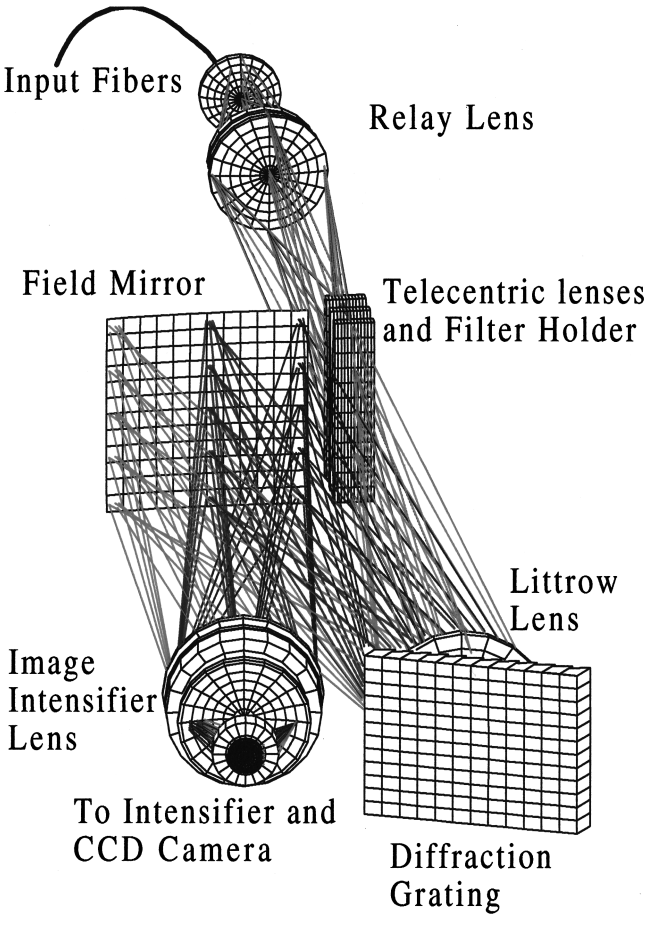

FIG. 2. Spectrometer drawing.

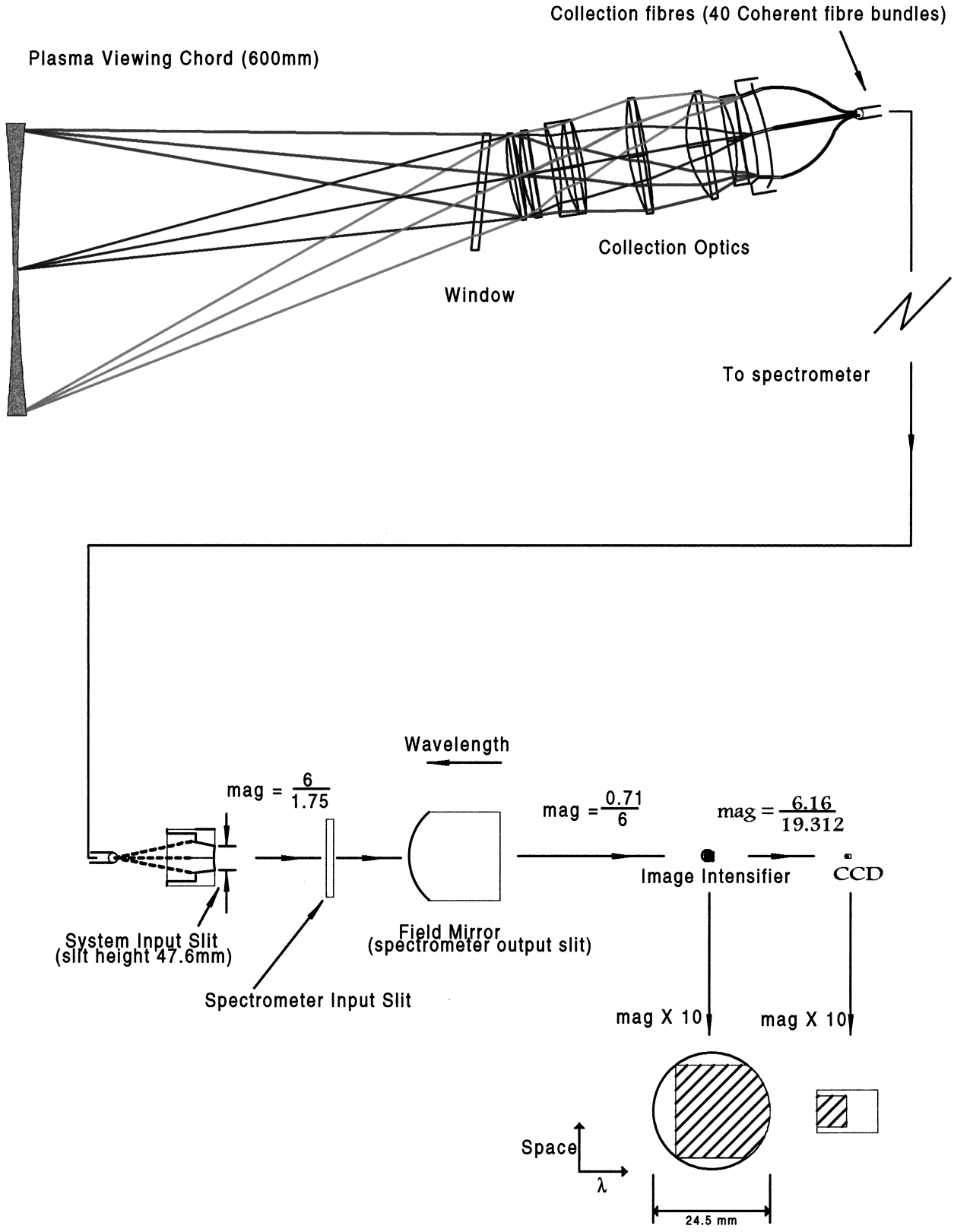

FIG. 3. Sketch of overall system.

both stages the intrinsic FOV is relatively narrow, i.e., ±7.5° and ±5.7°, for input and output relay stages and this, combined with the high numerical aperture requirements equivalent to f/1.35 and f/0.63 for an object at infinity, suggests a Petzval Lens configuration (two positive power groups separated by a distance of 50%–75% of the focal length) as the natural choice for both input (I/P) and output (O/P) applications.

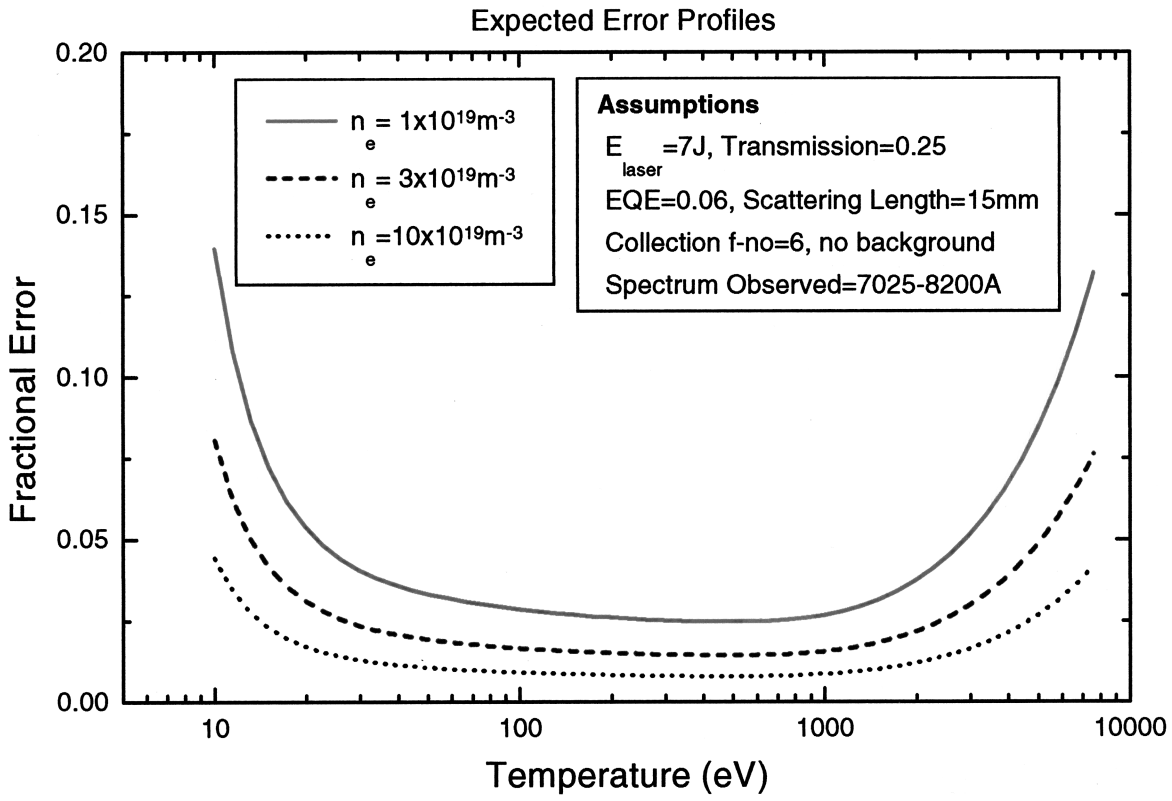

FIG. 4. Error calculations for varying densities as a function of temperature. This calculation was carried out without the effect of background light. Inclusion of background will tend to increase the errors generally and more rapidly at the low and high temperature ends.

The extreme *f* number of the final lens is dictated by the requirement to maximize the light onto the image intensifier (see below). The final element of the lens is optically connected to the image intensifier faceplate with an index matching fluid.

The image of the laser wavelength on the image intensifier is offset to one side (see Fig. 3). This gives a slightly restricted wavelength (temperature) range at the top and bottom of the image. However, these channels are at the plasma periphery where temperature and spectrum are narrower and the offset allows several more spatial channels at minimal extra expense.

V. MASKING/STRAY LIGHT REDUCTION

Consideration was also given to reduce the stray scattered light in the spectrometer to obtain the best possible contrast. The diffraction grating, Littrow lens, and field mirror are masked and oriented so that only the rays contained in the computed envelope are transmitted. We also utilize the fact that the ghost images of the input slit imaged from the front and back of the Littrow lens (secondary images) are well focused and this allows us to mask out the scatter from these surfaces with less than 5% of the light being lost. The instrument is mounted in a large light-tight room with blackened walls.

VI. IMAGE INTENSIFIER

It was found that a third generation (GaAs) image intensifier was the most suitable for our requirements. It has a turn-on/turn-off (10%–90%) time of less than 10 ns and its photocathode has a quantum efficiency of up to 30% in the red end of the spectrum (600–850 nm) and an overall effective quantum efficiency[5] ($EQE = QE/NF^2$) of approximately 6% (this includes the conducting under layer needed to achieve the fast gating). The phosphor is a high-efficiency P43, and has an approximate decay time (90%–10%) of 1 ms. The light emitted from the phosphor is primarily at 540 nm, and is well matched to the CCD response. This intensifier allowed the use of the spectrally cleaner red end of the spectrum.

VII. CCD CAMERA

The CCD camera is a Peltier cooled, back-illuminated, frame-transfer type, scientific grade CCD chip with 576 $\times$384 pixel. Half of these pixels are used for storage giving 288$\times$384 usable pixels. Each pixel is 22 μm square giving an active area of 6.3 mm$\times$8.4 mm (half the chip). Each spatial channel occupies 7$\times$280 pixels. The vertical transfer rate per row is 0.65 μs and hence to clock down all 288 rows takes 188 μs. Thus with on chip binning, many temperature and density profiles could be acquired with time resolutions as fast as 188 μs (assuming the image intensifier has a sufficiently fast phosphor). The total readout time of the chip is approximately 1.15 s in the fast mode and 7.5 s in the slow (lower adc noise) mode. The CCD chip has a quantum efficiency of approximately 71% in the green (which gives a good matching to the wavelength at which the intensifier

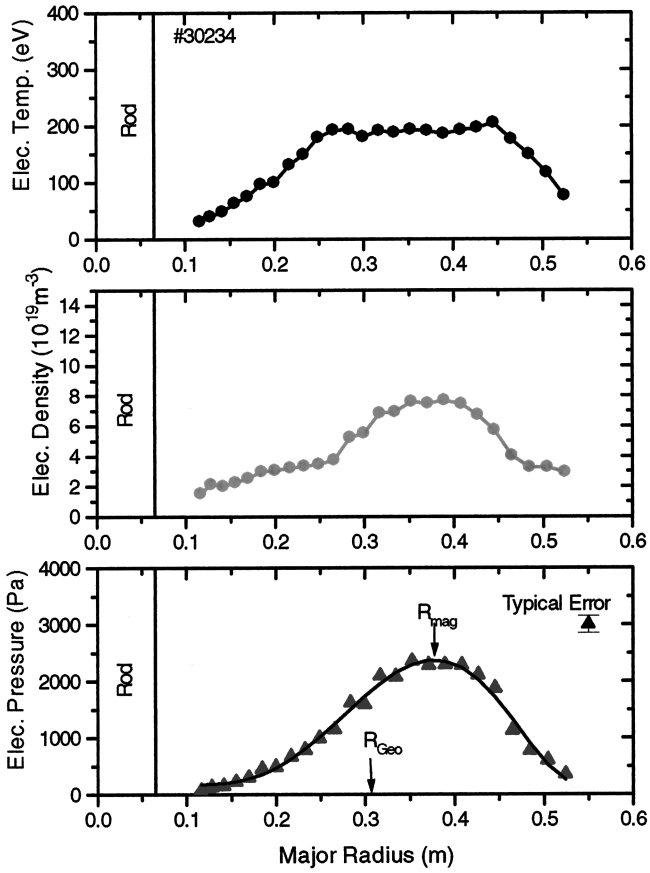

FIG. 5. Electron temperature, density, and pressure profiles in a typical START shot.

mainly emits). The readout noise from the CCD camera is 4.8 electrons root mean square (rms) where the reciprocal gain is 2.5 electrons/count.

VIII. IMAGE INTENSIFIER TO CCD LIGHT COUPLING

The purpose of the image intensifier is purely to act as a fast gate. Unfortunately it handicaps the quantum efficiency performance, i.e., 6% EQE as opposed to the 70%–80% EQE from the back-illuminated CCD chip. However, without a gate, the shot noise on the background light from the plasma would completely obliterate the scattered signal and hence the image intensifier is a necessity with present day CCD technology. Since the image intensifier has a phosphor backplane, a method of efficiently extracting the Thomson scattering data has to be used. In this case, we chose to use a CCD. To couple the CCD and image intensifier together, there is a choice of a fiber stub or a lens solution. The fiber system is more compact, while the lens coupling is more bulky. On the other hand, however, the fiber coupling is intricately linked with the CCD build while the lens solution is flexible and can utilize back-illuminated CCD chips. We use the lens solution.

In the START system, a Canon 80–200 nm f/1.8 was coupled with a Rodenstock f/0.75 to form a conjugate pair. This allowed flexibility in achieving the required demagnification between the image intensifier and the CCD (about 3.13). This in conjunction with the back-illuminated chip gave us a performance which is estimated to be 1.5 times more efficient than fiber coupling. Overall, the cross talk between adjacent channels is typically 4%, which is negligible.

IX. RESULTS AND DISCUSSION

The 40 available fiber bundles are divided into 30 spatial and ten background channels. The ten background channels are organized to look just above the scattering volume and are equally spaced along it. In general, we find that the background light is extremely low over the time of observation. The low stray light levels in the system means that the electron density can easily be calibrated using Rayleigh Scattering from nitrogen. Figure 4 shows the results of detailed calculation of the errors for the system for a range of densities and temperatures. The accuracy, depending on plasma parameters, is typically from 2% on electron temperature. Figure 5 shows typical profiles of electron temperature and density and pressure for a START shot (No. 30234).

ACKNOWLEDGMENTS

This work is funded by the U.K. Department of Trade and Industry and Euratom. We are indebted to P.G. Carolan (Culham) for stimulating discussions and support during the project.

[1] M. J. Walsh, and R. J. Akers, *et al.*, Proceedings of the 23rd EPS Conference on Controlled Fusion and Plasma Physics, Kiev, 1996, Vol. 20C, Part 1, p. 425.
[2] N. Bretz, D. Dimock, V. Foote, D. Johnson, D. Long, and E. Tolnas, Appl. Opt. **17**, 192 (1978).
[3] C. J. Barth, M. L. P. Dirkx, B. J. J. Grobben, G. C. H. M. Verhaag, A. T. M. Wilbers, and A. J. Donné, Rev. Sci. Instrum. **63**, 4947 (1992).
[4] M. Laikin, *Lens Design* (Dekker, New York, 1995).
[5] R. J. Hertel, *Ultrahigh Speed Photography, Photonics and Videography '89* (SPIE, Bellingham, WA, 1989), pp. 332-343.